GMR
The Original

FABRICATION OF MULTISCALE STARCH/PVA/CaO ELECTROSPUN NANOSCAFFOLDS FROM *Sargassum ilicifolium* (BROWN MARINE MACROALGAE) EXTRACT: PHYSIOCHEMICAL CHARACTERIZATION AND WOUND HEALING ASSESSMENT ON HaCaT CELLS

Akilandeswari Thirugnanasambandam, Mani Panagal*

*Department of Biotechnology, Annai College of Arts and Science (Affiliated to Bharathidasan University), Kovilacheri, Kumbakonam-612503, Tamil Nadu, India. Email: aki.akila21@gmail.com; master.maniji@gmail.com
Correspondence: master.maniji@gmail.com (M.P.)

ABSTRACT
The fabrication of bioactive electrospun nanofibrous scaffolds is an effective approach to promote the healing of skin wounds as well as the adhesion, proliferation and regeneration of cells and tissues by imitating the microenvironment of ECM. Multiscale starch/poly(vinyl alcohol) (PVA)/calcium oxide (CaO) electrospun nanoscaffolds containing *Sargassum ilicifolium* extract were fabricated by electrospinning for potential application in wound healing. *Sargassum ilicifolium* is a brown marine macroalga that is rich in natural polysaccharides, polyphenols, flavonoids, and antioxidant materials that have antimicrobial, anti-inflammatory, and tissue-regenerative properties. The fabricated nanoscaffolds were characterized using scanning electron microscopy (SEM), Fourier-transform infrared spectroscopy (FTIR), X-ray diffraction (XRD), ultraviolet-visible (UV-Vis) spectroscopy, thermogravimetric analysis (TGA), differential scanning calorimetry (DSC), contact angle, tensile strength, swelling and degradation to investigate the morphology, chemical reactivity, crystallinity, thermal stability, hydrophilicity, tensile strength, swelling ratio and biodegradation of the fabricated nanoscaffolds. The morphology of the bead-free nanofibers on the continuous porous structure was observed through SEM. The FTIR analysis indicated successful immobilization of marine extract and CaO into starch/PVA composite scaffolds. XRD analysis indicated semi-crystalline nature of the composite scaffold, while thermal studies demonstrated that CaO nanoparticle reinforcement improved the thermal stability of the scaffold. The biological performance of prepared scaffolds was studied by cytocompatibility test and in vitro scratch wound healing assay by HaCaT cells. Obtained results revealed that composite nanoscaffolds supported excellent cell viability. Migration of keratinocytes was considerably superior in composite nanoscaffolds as compared to control group indicating better wound closure.

KEYWORDS: Green synthesis: Calcium oxide nanoparticles; *Sargassum ilicifolium*: Electrospun nanoscaffolds; Wound healing.

1. INTRODUCTION

Skin is the largest organ of the human body and serves as the primary barrier against microbial invasion, dehydration, ultraviolet radiation, and mechanical injury. When this barrier is disrupted by trauma, burns, diabetic ulcers, or chronic infection, the normal healing process may be delayed or impaired, increasing the risk of complications and reducing quality of life [1-4]. Wound healing is a complex biological process that involves hemostasis, inflammation, proliferation, and remodeling. Successful repair requires coordinated cell migration, extracellular matrix deposition, angiogenesis, and re-epithelialization. In chronic wounds, however, these events are often disrupted by persistent inflammation, bacterial contamination, oxidative stress, and reduced cellular activity [5, 6]. As a result, there is a growing need for advanced wound dressings that not only protect the wound surface but also actively promote tissue regeneration. Electrospinning has emerged as one of the most effective techniques for fabricating nanofibrous scaffolds for wound healing and tissue engineering. Electrospun materials closely resemble the native extracellular matrix because of their high surface area, interconnected porosity, and tunable fiber morphology [7]. These features support oxygen exchange, nutrient transport, moisture retention, and cell infiltration, all of which are essential for skin regeneration. In addition, electrospinning allows the incorporation of natural polymers, inorganic nanoparticles, and bioactive compounds into a single scaffold, making it possible to design multifunctional wound dressings with improved biological performance [8].

Among natural polymers, starch is an attractive material because it is abundant, inexpensive, biodegradable, and non-toxic. However, native starch has limited mechanical strength and poor electrospinnability, which restrict its direct use in scaffold fabrication. To overcome these limitations, starch is often blended with poly (vinyl alcohol) (PVA), a hydrophilic synthetic polymer known for its excellent film-forming ability, flexibility, and ease of electrospinning [9-12]. The combination of starch and PVA can improve solution processability, fiber formation,

and structural stability while maintaining biocompatibility. Such polymer blends are therefore suitable candidates for developing wound dressing materials with favorable physical and biological properties. Inorganic nanoparticles can further enhance the functionality of electrospun scaffolds. Calcium oxide (CaO) nanoparticles are of particular interest because of their antimicrobial activity, bioactivity, and ability to improve thermal and mechanical properties [13]. In wound healing applications, calcium ions play an important role in cell signaling, proliferation, and extracellular matrix synthesis. The incorporation of CaO into polymeric scaffolds may therefore contribute not only to improved material performance but also to enhanced biological responses at the wound site. When properly dispersed within a polymer matrix, CaO nanoparticles can strengthen the scaffold and support a more favorable environment for tissue repair [14, 15].

Marine macroalgae are another promising source of bioactive compounds for biomedical applications. *Sargassum ilicifolium*, a brown seaweed widely found in coastal regions, contains a variety of biologically active constituents such as polysaccharides, phenolic compounds, flavonoids, carotenoids, and sulfated metabolites [16, 17]. These compounds are known for their antioxidant, anti-inflammatory, and antimicrobial properties. In the context of wound healing, antioxidant molecules can help reduce excessive reactive oxygen species, which are commonly elevated in chronic wounds and can damage cells and delay repair [18]. In addition, marine-derived polysaccharides and phenolics may stimulate fibroblast activity, collagen deposition, and re-epithelialization, thereby supporting the healing process. Because of these properties, *Sargassum ilicifolium* extract is a promising natural additive for bioactive wound dressing systems [19-22].

The integration of *Sargassum ilicifolium* extract with starch/PVA/CaO electrospun scaffolds offers a synergistic approach to wound healing. In such a composite system, starch and PVA provide the structural framework, CaO contributes mechanical reinforcement and bioactivity, and the seaweed extract supplies antioxidant and therapeutic compounds [23]. Together, these components may produce a scaffold that is not only physically stable but also biologically active, hydrophilic, and supportive of cell growth and migration. This combination is particularly relevant for skin tissue engineering, where both material properties and cellular responses are critical for successful regeneration. Despite increasing interest in electrospun wound dressings, studies on multicomponent starch/PVA/CaO scaffolds loaded with *Sargassum ilicifolium* extract remain limited. Most reported systems focus on either synthetic polymers or single bioactive additives, whereas fewer investigations have explored the combined effects of marine extracts and inorganic nanoparticles within a biodegradable polymer matrix [24-26]. Developing such a scaffold could provide a sustainable and cost-effective alternative for advanced wound care, especially for chronic and difficult-to-heal wounds [27]. In this study, multiscale starch/PVA/CaO electrospun nanoscaffolds incorporated with *Sargassum ilicifolium* extract were fabricated and evaluated for wound healing applications. The scaffolds were characterized using scanning electron microscopy (SEM), Fourier transform infrared spectroscopy (FTIR), X-ray diffraction (XRD), UV–Visible spectroscopy, thermal analysis, contact angle measurement, tensile testing, swelling behavior, and degradation studies. In addition, their biological performance was assessed using HaCaT human keratinocyte cells through cytocompatibility and scratch wound healing assays. The aim of this work was to develop a multifunctional electrospun scaffold with improved physicochemical properties and enhanced potential for skin tissue engineering and wound repair.

2. MATERIALS AND METHODS

2.1. Collection and preparation of marine macroalgae

Brown macroalgae *S. ilicifolium* were manually gathered from the intertidal shores near Rameswaram, India. On arrival, samples were rinsed under flowing tap water to eliminate surface sand, debris, and epiphytes, followed by repeated washes with distilled water for complete purification. Cleaned algal material was chopped into smaller fragments and air-dried under shaded conditions at ambient temperature for approximately two weeks. The dried biomass was converted into fine powder and stored in airtight container at ambient conditions for further use in extraction.

2.2. Ultrasonic-assisted extraction of bioactive compounds

To extract bioactive constituents, 5 grams of the powdered *S. ilicifolium* were mixed with 100 mL of Milli-Q water. The mixture underwent sonication using a LABQUEST ultrasonic cleaner at 60°C for 45 minutes to enhance cell wall disruption and intracellular release. After sonication, the mixture was passed through sterile Whatman No. 1 filter paper to remove particulate matter, resulting in a clear extract. This filtrate was stored at 10°C for immediate use and subjected to lyophilization to obtain a dry extract powder for subsequent nanoparticle synthesis [28].

2.3. Green Synthesis of Calcium Oxide Nanoparticles

Calcium oxide (CaO) nanoparticles were synthesized through an environmentally friendly approach using a natural plant or marine algal extract as the reducing and stabilizing agent. Fresh biomass was thoroughly washed with distilled water, shade-dried, and ground into a fine powder. A calcium precursor solution was then prepared and slowly mixed with the extract under continuous magnetic stirring. During the reaction, phytochemicals such as phenolics, flavonoids, proteins, and polysaccharides facilitated the conversion of calcium ions into calcium-based nanoparticles while preventing particle aggregation. The resulting mixture was allowed to react completely, after which the precipitate was collected by centrifugation and repeatedly washed with distilled water and ethanol to remove residual impurities. The purified material was dried in a hot-air oven and subsequently calcined at an appropriate temperature to obtain crystalline calcium oxide nanoparticles. This green synthesis strategy eliminates

the need for hazardous chemicals, minimizes environmental impact, and produces biocompatible CaO nanoparticles suitable for biomedical, antimicrobial, and tissue engineering applications [29].

2.4. Preparation of starch/PVA/CaO electrospinning Solution

A starch solution (2 g) was prepared by dissolving starch in distilled water under continuous magnetic stirring at 50-80°C until complete gelatinization. Separately, PVA (10 g) was dissolved in distilled water by heating at 70-75°C with constant stirring until a homogeneous transparent solution was obtained. The starch and PVA solutions were mixed in the desired ratio and stirred continuously to obtain a uniform polymer blend. CaO nanoparticles were dispersed in distilled water using ultrasonication for 45 min to minimize particle agglomeration before being added to the polymer mixture. The predetermined amount of *Sargassum ilicifolium* (20ml) extract was then incorporated into the starch/PVA/CaO blend under continuous stirring. The final electrospinning solution was stirred for 2.5 h to ensure complete homogenization. Allow the solution to cool at room temperature and degas for 30 minutes [30].

2.5. Fabrication of Electrospun Nanoscaffolds

Electrospun nanoscaffolds were prepared using a laboratory-scale electrospinning apparatus. The prepared polymer solution was loaded into a syringe fitted with a stainless-steel needle connected to a high-voltage power supply. It was performed under optimized conditions at an applied voltage of 18 kV, a solution flow rate of 0.5 mL h^{-1}, and a tip-to-collector distance of 15 cm. The nanofibers were collected on an aluminium foil-covered rotating collector operating under ambient laboratory conditions (25 ± 2 °C and relative humidity of 45–55%). The collected nanofibrous mats were carefully peeled from the collector and dried under vaccum at room temperature for 24 hours to remove residual moisture before being stored in a desiccator for subsequent characterization and biological evaluation [31].

2.6. Physicochemical characterization of nanoparticles

2.6.1. UV-visible spectroscopy

UV-Visible spectroscopy was performed to confirm the incorporation of the bioactive extract and to investigate optical absorption characteristics of the fabricated nanoscaffolds. Spectra were recorded within the wavelength range of 200-800 nm using a UV-Visible spectrophotometer [32].

2.6.2. Fourier Transform Infrared Spectroscopy (FTIR)

FTIR analysis was carried out to identify the functional groups present in the scaffolds and to evaluate molecular interactions among starch, PVA, CaO, and *Sargassum ilicifolium* extract. Spectra were collected in the range of 4000-400 cm^{-1} using the attenuated total reflectance (ATR) mode [33].

2.6.3. X-Ray Diffraction (XRD)

The crystalline structure of the electrospun nanoscaffolds was analyzed using X-ray diffraction with Cu-Kα radiation (λ = 1.5406 Å). Diffraction patterns were recorded over a 2θ range of 10°-80° at a scanning rate of 2° min^{-1} under an operating voltage of 40kV and a current of 30mA. The obtained diffraction patterns were analysed to determine the crystalline phase and evaluate the effect of CaO nanoparticles and *Sargassum ilicifolium* extract on the crystallinity of the starch/PVA electrospun nanoscaffolds [34].

2.6.4. Scanning Electron Microscopy (SEM)

Surface morphology and fiber architecture were examined using scanning electron microscopy. Prior to imaging, samples were sputter-coated with a thin conductive layer of gold. Average fiber diameters were determined by measuring randomly selected fibers from SEM micrographs using image analysis software [35].

2.6.5. Thermogravimetric Analysis (TGA)

The thermal stability and degradation behavior of the electrospun starch/PVA/CaO nanoscaffolds incorporated with *Sargassum ilicifolium* extract were evaluated using a thermogravimetric analyzer. Approximately **5–10 mg** of each dried scaffold sample was placed in an alumina crucible and heated from **30 °C to 600 °C** at a **heating rate of 10 °C min^{-1}** under a continuous nitrogen atmosphere with a flow rate of **20 mL min^{-1}.** The percentage weight loss as a function of temperature was recorded to assess moisture evaporation, decomposition of the polymer matrix, degradation of the incorporated bioactive compounds, and the residual inorganic CaO content. The thermogravimetric curves were further analyzed to determine the thermal stability of the fabricated nanoscaffolds [36].

2.6.6. Zeta potential and particle size

The hydrodynamic particle size distribution and zeta potential of the green-synthesized calcium oxide (CaO) nanoparticle were determined using a dynamic light scattering (DLS) particle size analyser equipped with dispersed in deionized water at an appropriate concentration and ultrasonicated for 15 min to obtain a homogenous suspension. The particle size was measured at 25 **°C with a detection angle of 173°, and the average hydrodynamic diameter and polydispersity index (PDI) were recorded. Zeta potential measurements were performed using the electrophoretic light scattering technique at 25°C to evaluate the surface charge and colloidal stability of the nanoparticles. Each measurement was carried out in triplicate, and the results were expressed as the mean** ± standard deviation [37].

2.7. *In Vitro* Scratch Wound Healing Assay

The wound healing potential of *Sargassum ilicifolium* extract, green-synthesized CaO nanoparticles, and starch/PVA/CaO electrospun nanoscaffolds was evaluated using an in vitro scratch assay with HaCaT human keratinocyte cells. Cells were seeded in 6-well culture plates at a density of 2×10^5 cells per well in Dulbecco's Modified Eagle Medium (DMEM) supplemented with 10% fetal bovine serum (FBS) and 1% penicillin–

streptomycin. The cells were incubated at 37 °C in a humidified atmosphere containing 5% CO_2 until approximately 90–100% confluence was reached. A sterile 200 µL pipette tip was used to create a straight scratch across the cell monolayer. Detached cells were removed by gently washing the wells with phosphate-buffered saline (PBS), followed by the addition of serum-free DMEM containing different concentrations of the test samples (6.25, 12.5, 25, 50, and 100 µg mL^{-1}). Untreated cells maintained in serum-free DMEM served as the negative control. Images of the scratched region were captured at 0, 24, and 48 h using an inverted phase-contrast microscope. The percentage of wound closure was quantified using ImageJ software by comparing the wound area at each time point with the initial wound area [38].

2.8. Statistical analysis

All experiments were performed in triplicate unless otherwise stated. Data are presented as mean ± standard deviation (SD). Statistical analysis was carried out using GraphPad Prism or SPSS software. Differences among groups were evaluated using one-way analysis of variance (ANOVA) followed by an appropriate post hoc test. A value of $p < 0.05$ was considered statistically significant [39].

3. RESULTS

3.1. UV-Visible Spectroscopy

The optical characteristics of the green-synthesized calcium oxide (CaO) nanoparticles were investigated using UV–Visible spectroscopy in the wavelength range of 200–800 nm, and the corresponding spectrum is shown in Fig. 1. The spectrum exhibited a distinct absorption maximum at approximately 304 nm with an absorbance of **0**.878, indicating the successful formation of CaO nanoparticles. The absorption band observed in the ultraviolet region is attributed to the electronic transitions associated with the Ca–O lattice and is considered a characteristic feature of nanosized calcium oxide. The appearance of this well-defined absorption peak confirms the conversion of the calcium precursor into CaO nanoparticles through the green synthesis process. Following the absorption maximum, the absorbance gradually decreased with increasing wavelength and extended smoothly into the visible region without the appearance of any additional absorption bands. This gradual decline suggests that the synthesized nanoparticles possess good optical purity and are free from significant secondary phases or unwanted reaction by-products [40].

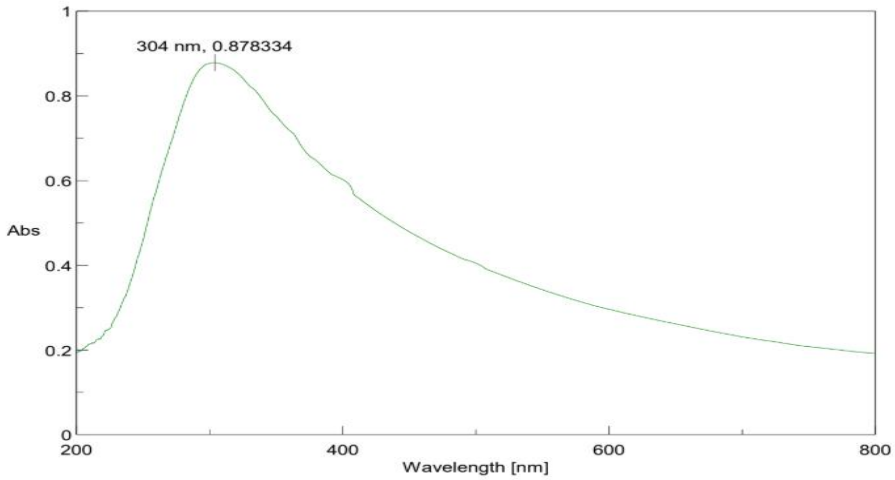

Fig 1. UV-Visible spectrum of Cao nanoparticles synthesized using *Sargassum ilicifolium* extract

The broad absorption profile may also be associated with the nanoscale dimensions of the particles and the presence of bioactive phytochemicals from *Sargassum ilicifolium*, which act as natural reducing and stabilizing agents during nanoparticle synthesis. The successful synthesis of CaO nanoparticles can be attributed to the phytochemical constituents of *Sargassum ilicifolium*, including polyphenols, flavonoids, and polysaccharides, which facilitate the reduction of calcium ions while simultaneously preventing excessive particle aggregation through surface capping. The absence of noticeable absorption peaks in the visible region further indicates that the synthesized nanoparticles are well dispersed and exhibit good stability. Overall, the UV–Visible spectral analysis confirms the successful green synthesis of CaO nanoparticles using *Sargassum ilicifolium* extract. The characteristic absorption peak at 304 nm**,** together with the smooth absorption profile and lack of impurity-related peaks, demonstrates the formation of stable CaO nanoparticles suitable for subsequent incorporation into starch/PVA electrospun nanoscaffolds for antimicrobial and biomedical applications [41].

3.2. FTIR Analysis

The FTIR spectra of green-synthesized CaO nanoparticles and starch/PVA/CaO electrospun nanofibers were recorded from 4000-400 cm^{-1} (Fig 2). The nanofiber spectrum showed a broad band at 3200-3400 cm^{-1}, assigned to O-H stretching from starch, PVA, and *Sargassum ilicifolium* phytochemicals, indicating strong hydrogen bonding. The peak near 2900 cm^{-1} corresponds to aliphatic C-H stretching, while the band around 1640 cm^{-1} is related to O–H bending of adsorbed water and possible C=O vibrations from phenolic compounds. Bands at 1400-1450 cm^{-1} are attributed to C-H bending and carboxylate groups, and peaks between 1000 and 1150 cm^{-1} arise from C-O-C and C-O stretching of starch and PVA. In the CaO nanoparticle spectrum, characteristic bands below

900 cm^{-1}, especially in the 500–700 cm^{-1} region, confirm Ca-O stretching and successful CaO formation. Minor shifts and intensity changes in the composite nanofibers suggest interactions among the polymer matrix, CaO nanoparticles, and seaweed-derived phytochemicals. FTIR confirms the presence of functional groups from starch, PVA, *Sargassum ilicifolium* and CaO demonstrating successful fabrication of bioactive starch/PVA/CaO electrospun nanoscaffolds [42].

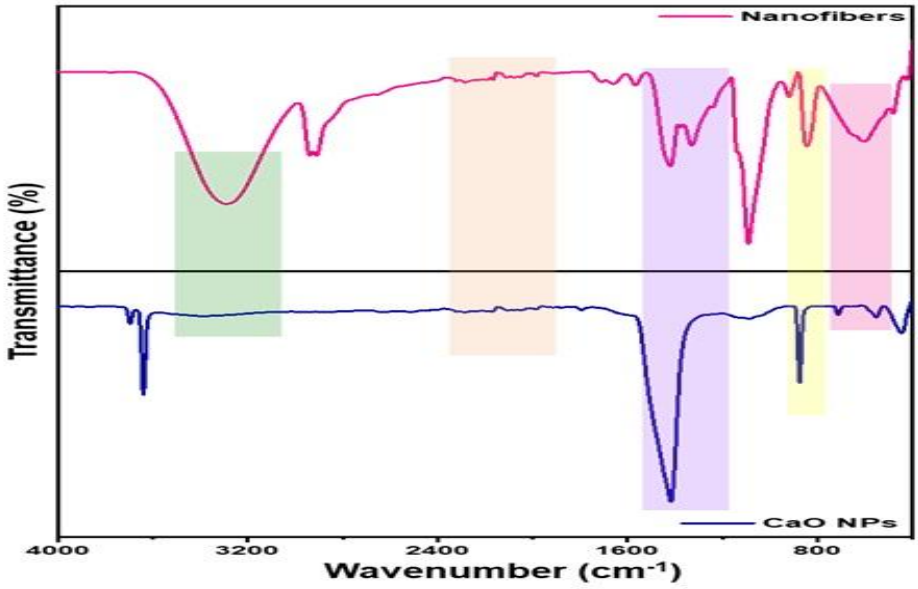

Fig 2. FTIR Spectra of CaO nanoparticles and electrospun nanofiber incorporating *Sargassum ilicifolium* extract

3.3. XRD Analysis

The crystalline characteristics of the green-synthesized CaO nanoparticles and starch/PVA/CaO electrospun nanofibers were investigated using X-ray diffraction (XRD), and the diffraction patterns are presented in Fig 3. The XRD pattern of the CaO nanoparticles exhibited distinct diffraction peaks at approximately 2θ = 18°, 29°, 32°, 36°, 50°, 54°, 58°, 64°, and 67°, indicating the crystalline nature of the synthesized calcium oxide nanoparticles. The prominent diffraction peaks observed around 32°, 37°, 54°, 64°, and 67° are characteristic reflections of crystalline CaO, confirming the successful formation of the metal oxide phase. The sharp and intense diffraction peaks indicate good crystallinity of the green-synthesized nanoparticles. The XRD pattern of the starch/PVA/CaO electrospun nanofibers exhibited a broad diffraction halo in the low-angle region (approximately 15-25°), which is characteristic of the semi-crystalline nature of the starch/PVA polymer matrix. In addition, distinct diffraction peaks corresponding to CaO were retained within the composite nanofibers, although their intensities were reduced and slightly broadened due to the homogeneous dispersion of nanoparticles within the polymer network. The reduction in peak intensity and slight peak broadening suggest strong interactions between the polymer chains, CaO nanoparticles, and the bioactive constituents of *Sargassum ilicifolium* extract [43].

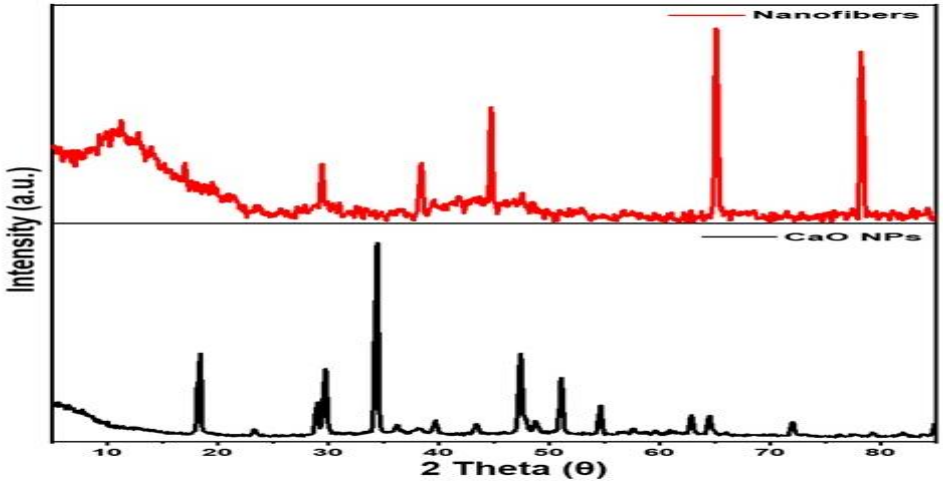

Fig 3. XRD patterns of synthesized CaO NPs and Nanofibers

No additional diffraction peaks corresponding to secondary crystalline impurities were observed, indicating the high phase purity of the synthesized CaO nanoparticles and their successful incorporation into the electrospun scaffold. The coexistence of the semi-crystalline polymer matrix and crystalline CaO nanoparticles demonstrates the formation of a stable composite nanofibrous scaffold with improved structural integrity. These findings

confirm the successful fabrication of starch/PVA/CaO electrospun nanoscaffolds and support their potential application as bioactive wound dressing materials [44].

3.4. SEM Analysis

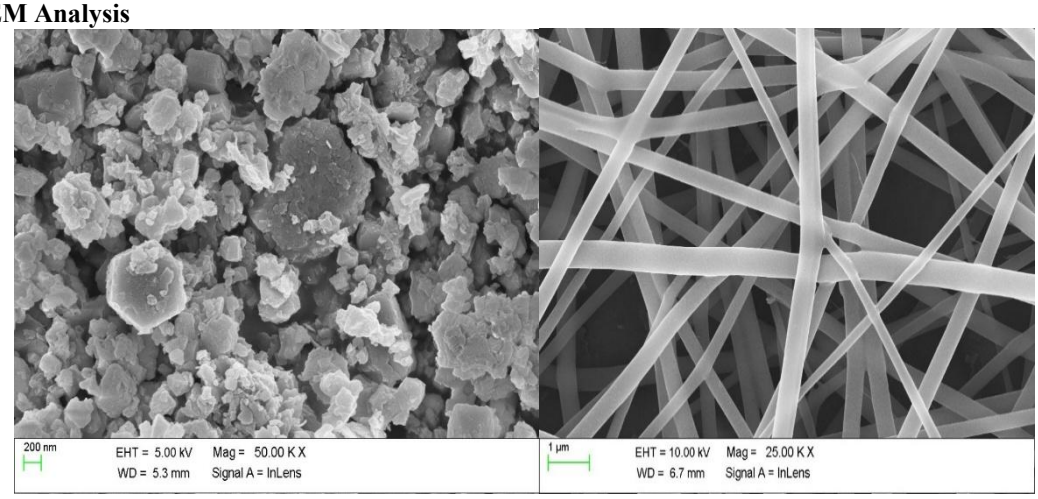

Fig 4. SEM analysis of synthesized CaO NPs and loaded starch/PVA electrospun nanoscaffolds

Scanning electron microscopy (SEM) was used to examine the morphology of the green-synthesized CaO nanoparticles and the fabricated starch/PVA/CaO electrospun nanoscaffold. As shown in Fig 4, the CaO nanoparticles appeared as irregularly shaped particles with slight agglomeration. This aggregation is commonly observed in metal oxide nanoparticles due to their high surface energy during drying. Nevertheless, the particles were uniformly distributed, indicating that the *Sargassum ilicifolium* extract effectively facilitated the green synthesis of CaO nanoparticles. Their nanoscale structure provides a large surface area, which is beneficial for improving the biological performance of the scaffold. The SEM image of the starch/PVA/CaO electrospun nanoscaffold revealed a dense network of smooth, continuous, and randomly oriented nanofibers with no obvious bead formation. The fibers were interconnected, creating a porous architecture similar to the natural extracellular matrix of skin tissue. Such a structure is advantageous for wound healing because it supports oxygen exchange, nutrient diffusion, and cell attachment while allowing efficient migration and proliferation of keratinocytes. In addition, no visible cracks or large nanoparticle aggregates were observed on the scaffold surface, suggesting that the CaO nanoparticles were well dispersed within the starch/PVA matrix. The SEM observations confirm the successful fabrication of a uniform electrospun nanoscaffold with desirable morphological features. The interconnected porous structure and homogeneous distribution of CaO nanoparticles indicate that the scaffold possesses the structural characteristics required for wound dressing and skin tissue engineering applications [45].

3.5. TGA

The thermal stability of the green-synthesized CaO nanoparticles was evaluated using thermogravimetric analysis (TGA), and the corresponding thermogram is shown in Fig 5. The TGA curve demonstrated a gradual weight loss with increasing temperature, indicating the thermal behavior of the synthesized nanoparticles. A small weight loss was observed below 100 °C**,** which can be attributed to the evaporation of physically adsorbed moisture and other volatile compounds present on the nanoparticle surface. This initial loss was minimal, suggesting that the synthesized CaO nanoparticles contained only a small amount of residual water. The most significant weight loss occurred between approximately 220 and 300 °C, corresponding to the decomposition of organic compounds derived from the *Sargassum ilicifolium* extract. These bioactive molecules acted as natural reducing and stabilizing agents during the green synthesis process and gradually decomposed upon heating [46].

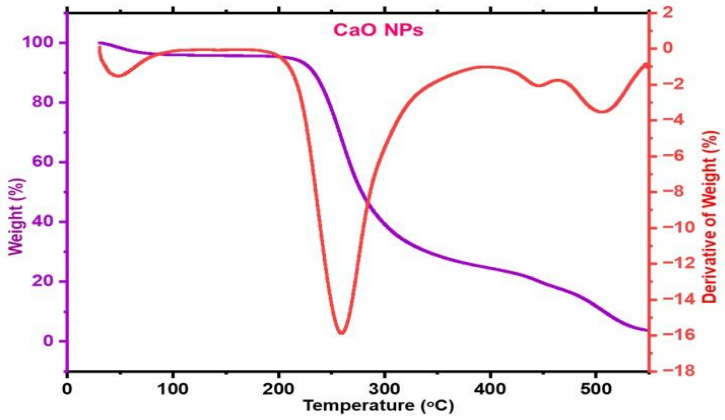

Fig 5. TGA behaviour of CaO Nanoparticles

The derivative thermogravimetric (DTG) curve exhibited a prominent peak at around 260 °C, indicating the maximum rate of thermal degradation. Beyond 300 °C**,** the rate of weight loss decreased considerably, and the thermogram became relatively stable up to 550 °C**.** A small additional weight loss observed at higher temperatures may be associated with the decomposition of trace organic residues or structural rearrangements within the material. The presence of a stable residual mass at the end of the analysis confirms the formation of thermally stable CaO nanoparticles. The TGA results demonstrate that the green-synthesized CaO nanoparticles possess good thermal stability after the removal of surface moisture and residual phytochemicals. This enhanced thermal behavior indicates that the nanoparticles are suitable for incorporation into starch/PVA electrospun nanoscaffolds intended for wound healing and tissue engineering applications [47].

3.6. Zeta Potential and CaO particle size analysis

The hydrodynamic particle size and surface charge of the green-synthesized CaO nanoparticles were evaluated using dynamic light scattering (DLS) and zeta potential analysis. The results demonstrated a Z-average particle size of 804 nm with a polydispersity index (PDI) of 0.5696, indicating a moderately broad particle size distribution. The relatively large hydrodynamic size compared to the nanoscale dimensions observed by SEM may be attributed to the aggregation of nanoparticles in the aqueous suspension during DLS measurement. Such differences are commonly observed because DLS measures the hydrated particle diameter, whereas SEM determines the size of dried individual particles. The intensity distribution revealed a dominant particle population centered around 759.2 nm, accounting for approximately 79.21% of the total particle population, together with a smaller fraction at 111.4 nm (16.64%) and a minor aggregated population at 5422 nm (4.16%). These results suggest that most of the nanoparticles formed stable aggregates in suspension while only a small proportion existed as larger agglomerates. The zeta potential of the synthesized CaO nanoparticles was determined to be −22.13 mV, indicating that the nanoparticle surface possessed a moderate negative charge. This negative surface potential is mainly attributed to the adsorption of bioactive compounds from *Sargassum ilicifolium* extract, which act as natural capping agents during the green synthesis process. The presence of these phytochemicals contributes to electrostatic repulsion between particles, thereby improving colloidal stability and reducing excessive aggregation. The particle size and zeta potential analyses confirm the successful formation of green-synthesized CaO nanoparticles. The moderately negative zeta potential together with the observed particle size distribution indicates that the nanoparticles possess acceptable colloidal stability and are suitable for incorporation into starch/PVA electrospun nanoscaffolds for wound healing applications [48].

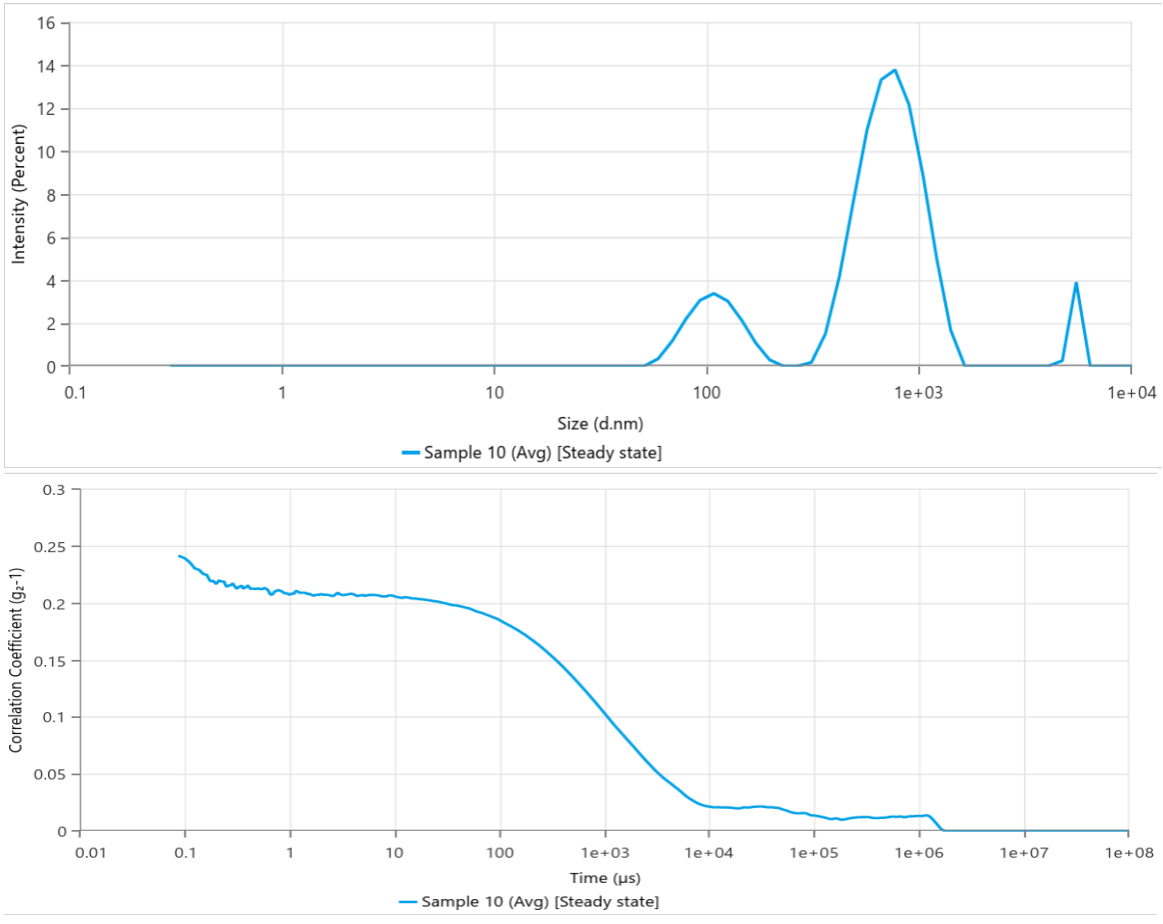

Fig 6. DLS particles size analysis of CaO NPa

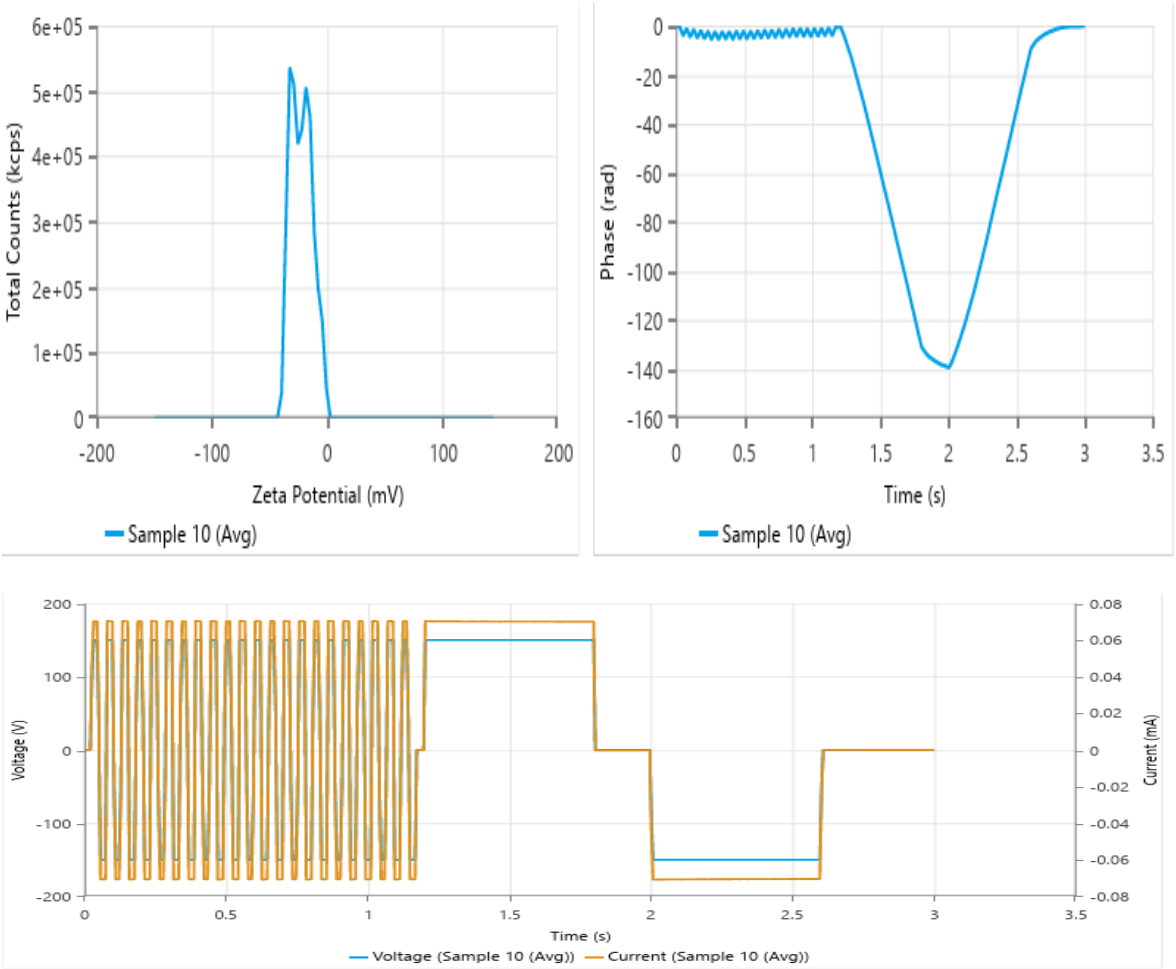

Fig 7. Zeta Potential of CaO NPs

3.7. Wound Healing (scratch) Assay

The wound healing ability of *Sargassum ilicifolium* extract, green-synthesized CaO nanoparticles, and starch/PVA/CaO electrospun nanoscaffolds was evaluated using an in vitro scratch assay on HaCaT cells. The percentage of wound closure at different treatment concentrations is presented in Fig 8. All treatment groups showed a concentration-dependent increase in wound closure when compared with the untreated control. The control group exhibited approximately 26% wound closure, indicating the normal migratory ability of HaCaT cells in the absence of treatment. Treatment with *Sargassum ilicifolium* extract resulted in a gradual improvement in wound healing, increasing from approximately 32% at 6.25 µg/mL to about 69% at 100 µg/mL. This enhancement may be attributed to the presence of naturally occurring bioactive compounds, including polyphenols, flavonoids, and polysaccharides, which are known to promote cell migration and tissue repair. The green-synthesized CaO nanoparticles also exhibited a dose-dependent increase in wound closure, with values rising from approximately 40% at 6.25 µg/mL to 83% at 100 µg/mL. The improved wound healing response may be associated with the bioactive nature of CaO nanoparticles, which can stimulate keratinocyte migration and create a favorable environment for tissue regeneration. Among all the treatment groups, the starch/PVA/CaO electrospun nanoscaffolds demonstrated the highest wound healing activity. Wound closure increased from approximately 47% at 6.25 µg/mL to nearly 95% at 100 µg/mL, indicating a significant enhancement in cell migration compared with both the extract and CaO nanoparticles alone. The superior performance of the nanoscaffold can be attributed to the combined effects of the porous electrospun structure, the sustained availability of CaO nanoparticles, and the bioactive phytochemicals from *Sargassum ilicifolium*. The nanofibrous architecture closely resembles the natural extracellular matrix, providing a suitable surface for cell attachment, proliferation, and migration while supporting efficient tissue regeneration.The scratch assay demonstrates that the starch/PVA/CaO electrospun nanoscaffold possesses superior wound healing potential compared with the algal extract and CaO nanoparticles alone, highlighting its promise as a bioactive wound dressing material for skin tissue engineering applications [49].

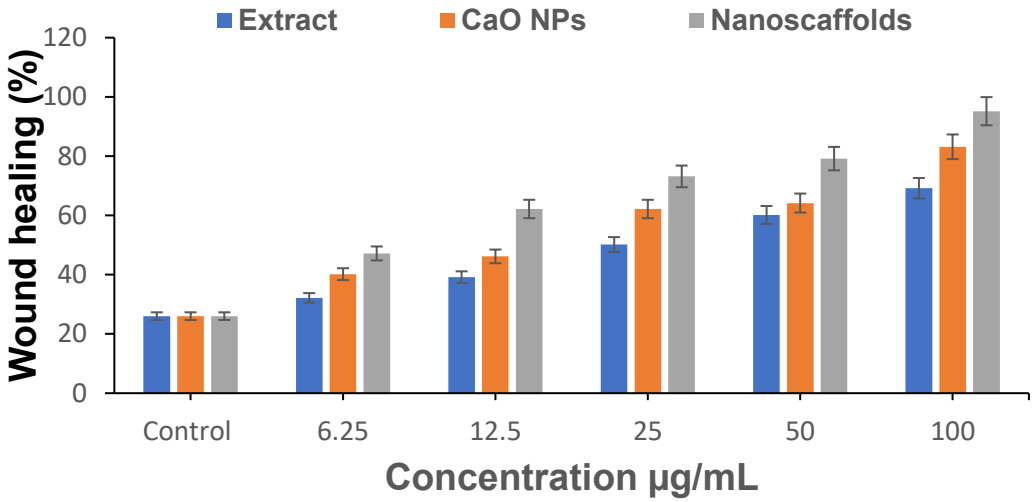

Fig 8. Wound healing activity analysis of algal extract, CaO NPs and stract/PVA/CaO NPs nanpscaffolds

4. DISCUSSION

The present study successfully demonstrated the fabrication of starch/PVA/CaO electrospun nanoscaffolds using green-synthesized calcium oxide nanoparticles obtained from *Sargassum ilicifolium* extract. The combination of a naturally derived polymer matrix with bioactive inorganic nanoparticles produced a multifunctional scaffold possessing desirable physicochemical characteristics and promising biological activity for wound healing applications. The findings indicate that incorporating CaO nanoparticles into the electrospun matrix not only improved the structural properties of the scaffold but also significantly enhanced its ability to promote keratinocyte migration.

UV–Visible spectroscopy provided the initial confirmation of CaO nanoparticle formation through the characteristic absorption band observed in the ultraviolet region. The absence of additional absorption peaks in the visible region suggests that the nanoparticles were synthesized without significant impurity phases. During green synthesis, the phytochemicals present in *Sargassum ilicifolium*, including polyphenols, flavonoids, and polysaccharides, likely acted as both reducing and stabilizing agents. These naturally occurring compounds play an important role in controlling nanoparticle formation while minimizing the use of hazardous chemicals, making the synthesis process environmentally friendly and suitable for biomedical applications [50-56].

The FTIR analysis further confirmed the successful interaction between the polymer matrix, CaO nanoparticles, and the bioactive constituents of the algal extract. The broad hydroxyl absorption band and the characteristic Ca–O vibration demonstrated that the nanoparticles were effectively incorporated into the starch/PVA matrix without altering the essential chemical structure of the polymers. Slight changes in peak intensity and position indicate the formation of intermolecular hydrogen bonding between starch, PVA, and the phytochemicals present in the extract. Such molecular interactions contribute to improved compatibility between the organic and inorganic components, resulting in a stable composite scaffold [57-61].

The crystalline nature of the synthesized nanoparticles was confirmed through X-ray diffraction analysis. The diffraction peaks corresponding to crystalline CaO remained visible after electrospinning, indicating that the crystal structure of the nanoparticles was preserved during scaffold fabrication. At the same time, the broad diffraction halo associated with starch and PVA confirmed the semi-crystalline nature of the polymer matrix. The coexistence of crystalline CaO and the polymeric network suggests successful formation of a composite material with balanced mechanical integrity and structural stability. Preservation of crystallinity is particularly important because it contributes to the sustained biological performance of the incorporated nanoparticles [62-67].

SEM observations revealed clear differences between the morphology of the CaO nanoparticles and the fabricated electrospun scaffold. The green-synthesized nanoparticles appeared as irregular nanosized particles with slight aggregation, which is commonly observed in metal oxide nanoparticles due to their high surface energy. In contrast, the electrospun scaffold exhibited smooth, bead-free, and uniformly distributed nanofibers forming an interconnected porous network. This porous architecture closely resembles the extracellular matrix of native skin tissue and provides an ideal microenvironment for cell attachment, proliferation, nutrient diffusion, and gas exchange. The absence of visible defects and large nanoparticle agglomerates indicates that the electrospinning parameters and polymer composition were suitable for producing homogeneous nanoscaffolds. Dynamic light scattering analysis showed a larger hydrodynamic particle size than that observed in the SEM images. This difference is expected because DLS measures the hydrated particle diameter in suspension, whereas SEM measures the physical size of dried particles. The moderately negative zeta potential of −22.13 mV indicates that the CaO nanoparticles possess reasonable colloidal stability due to electrostatic repulsion generated by the phytochemical coating from *Sargassum ilicifolium*. These surface-bound biomolecules help minimize excessive aggregation and enhance nanoparticle dispersion within the polymer matrix during scaffold fabrication [68-73].

Thermogravimetric analysis demonstrated that the synthesized CaO nanoparticles possess good thermal stability. The initial weight loss observed at lower temperatures was attributed to the evaporation of physically adsorbed

moisture, while the major degradation stage corresponded to the decomposition of residual organic compounds originating from the algal extract. Beyond this stage, the thermogram became relatively stable, confirming the formation of thermally stable CaO nanoparticles. Good thermal stability is advantageous because it ensures that the nanoparticles retain their structural integrity during scaffold fabrication, sterilization, and biomedical use [74-77].

The biological performance of the fabricated scaffold was evaluated using an in vitro scratch wound healing assay on HaCaT keratinocyte cells. All treatment groups demonstrated concentration-dependent wound closure; however, the starch/PVA/CaO electrospun nanoscaffold consistently exhibited the highest wound healing activity. At the highest concentration, the nanoscaffold achieved nearly complete wound closure, clearly outperforming the algal extract and CaO nanoparticles alone. This enhanced performance is likely due to the synergistic interaction between the bioactive compounds of *Sargassum ilicifolium*, the biological activity of CaO nanoparticles, and the extracellular matrix-like architecture of the electrospun scaffold. Together, these factors promote keratinocyte migration, facilitate cell adhesion, and support tissue regeneration. This finding demonstrate that combining green nanotechnology with electrospinning provides an effective strategy for developing advanced wound dressing materials [78-80]. The fabricated starch/PVA/CaO nanoscaffold integrates excellent physicochemical properties with superior biological performance, making it a promising candidate for skin tissue engineering and wound management. Although the present work confirms it *in vitro* potential, further studies involving antimicrobial evaluation, mechanical characterization, biocompatibility assessment, and in vivo wound healing models are necessary to validate its clinical applicability.

5. CONCLUSION

The present study successfully developed a bioactive starch/PVA/CaO electrospun nanoscaffold incorporating green-synthesized calcium oxide nanoparticles derived from *Sargassum ilicifolium* extract. The use of marine macroalgal extract as a natural reducing and stabilizing agent provided an environmentally friendly approach for nanoparticle synthesis while eliminating the need for hazardous chemicals. The fabricated nanoscaffold combined the advantages of natural polymers with the biological activity of CaO nanoparticles, resulting in a multifunctional material suitable for wound healing applications. Comprehensive physicochemical characterization confirmed the successful synthesis and incorporation of CaO nanoparticles into the electrospun scaffold. UV–Visible spectroscopy verified nanoparticle formation, while FTIR analysis demonstrated effective interactions between starch, PVA, CaO nanoparticles, and the phytochemicals present in the algal extract. XRD analysis confirmed the crystalline nature of CaO and the semi-crystalline structure of the polymer matrix. SEM images revealed a uniform, bead-free, interconnected fibrous network resembling the natural extracellular matrix, providing an ideal environment for cellular attachment and migration. Particle size and zeta potential analyses demonstrated acceptable colloidal stability, and thermogravimetric analysis confirmed that the synthesized nanoparticles possessed good thermal stability. The in vitro scratch wound healing assay demonstrated that the starch/PVA/CaO electrospun nanoscaffold significantly enhanced HaCaT cell migration compared with the algal extract and CaO nanoparticles alone. The concentration-dependent improvement in wound closure highlights the synergistic effect of the polymer matrix, bioactive phytochemicals, and calcium oxide nanoparticles in promoting tissue regeneration. The porous nanofibrous architecture further contributed to its excellent biological performance by mimicking the native extracellular matrix. The developed starch/PVA/CaO electrospun nanoscaffold represents a promising biomaterial for wound dressing and skin tissue engineering. Its environmentally friendly synthesis, favorable physicochemical characteristics, and enhanced wound healing activity demonstrate its potential for future biomedical applications. Further investigations involving mechanical characterization, antimicrobial studies, long-term cytocompatibility, and in vivo wound healing models will provide additional evidence for its translation into clinical wound care.

Funding statement: Not Available

Conflicts of Interest: The authors declare no conflicts of interest.

Ethics approval statement: Not Applicable

REFERENCES

[1] Kannappan P, Chandrasekaran MK, Raju MV, Gopalakrishnan S, Dhamodharan P, Ahalliya RM, Palanisamy CP, Raju B, Kanniappan GV. Exploring the anticancer potential of Jerantinine A from Tabernaemontana coronaria against prostate, breast, and ovarian cancers: a computational approach. Journal of Complementary and Integrative Medicine. 2025; 22(02): 363-372.

[2] Pei J, Kumarasamy RV, Jayaraman S, Kanniappan GV, Long Q, Palanisamy CP. Quercetin-functionalized nanomaterials: Innovative therapeutic avenues for Alzheimer's disease management. Ageing Research Reviews. 2025; 104: 102665.

[3] Jayaraman S, Prasad M, Natarajan SR, Krishnamoorthy R, Alshuniaber MA, Gatasheh MK, Veeraraghavan VP, Rajagopal P, Palanisamy CP. Molecular mechanisms underlying the effects of beta-sitosterol on TGF-β1/Nrf2/SIRT1/p53-mediated signaling in the kidney of a high-fat diet and sucrose-induced type-2 diabetic rat. Chemico-Biological Interactions. 2025; 411: 111443.

[4] Huang Y, Guo H, Liu Y, Jin W, Palanisamy CP, Pei J, Oz F, El-Aty AMA. Effects of Natural Polysaccharides on the Gut Microbiota Related to Human Metabolic Health. Molecular Nutrition & Food Research. 2025; e202400792.
[5] Prabhakaran P, Palanisamy CP, Shanmugam A, Damodharan P, Swaminathan H, Devaraj D, Ahalliya RM, Kanniappan GV. Isolation, structural characterization, and molecular docking studies on the bioactive compound from n-Hexane extract of Emilia sonchifolia (L.) DC against the pancreatic cancer target Aurora 2 Kinase. Journal of Complementary and Integrative Medicine. 2024; 22(1): 0290.
[6] Jiang H, Kumarasamy RV, Pei J, Raju K, Kanniappan GV, Palanisamy CP. Integrating engineered nanomaterials with extracellular vesicles: Advancing targeted drug delivery and biomedical applications. Frontiers in Nanotechnology. 2024; 6: 1513683.
[7] Guo H, Liu Y, Wan T, Song D, Palanisamy CP, Geng J, Pei J, Özmen S, El-Aty AMA. Toward personalized cancer management: Role of precision nutrition–diet interventions. Journal of Functional Foods. 2024; 123: 106584.
[8] Natarajan SR, Krishnamoorthy R, Alshuniaber MA, Al-Anazi KM, Farah MA, Rajagopal P, Palanisamy CP, Veeraraghavan VP, Jayaraman S. Identification of FOXM1 as a novel protein biomarker and therapeutic target for colorectal cancer progression: Evidence from immune infiltration and bioinformatic analyses. International Journal of Biological Macromolecules. 282 (Part 4): 137201.
[9] Rajendran MS, Jayaraman S, Khan JM, Jasmine S, Prabhakaran RK, Raju MV, Chandrasekaran MK, Ahalliya RM, Kannappan P, Palanisamy CP, Kanniappan GV. Investigating the colon toxicity and carcinogenic role of monosodium glutamate compared with Dimethylhydrazine in male Wistar rats: Exploring the link to childhood colon cancer risk. Journal of King Saud University - Science. 2024; 36(11): 103507.
[10] Kumarasamy RV, Natarajan P, Umapathy VR, Roy JR, Rab SO, Saeed M, Panagal M, Mironescu M, Srinivasan GP, Palanisamy CP. Clinical Applications and Therapeutic Potentials of Advanced Nanoparticles: A Comprehensive Review on Completed Human Clinical Trials. Frontiers in Nanotechnology. 2024; 6:1479993.
[11] Jin W, Pei JJ, Roy JR, Jayaraman S, Ahalliya RM, Kanniappan GV, Mironescu M, Palanisamy CP. Comprehensive review on single-cell RNA sequencing: A new frontier in Alzheimer's disease research. Ageing Research Reviews. 2024; 274: 102454.
[12] Pei J, Palanisamy CP, Jayaraman S, Natarajan PM, Umapathy VR, Roy JR, Panagal M, Jayaraman S. Curcumin-loaded polymeric nanomaterials as a novel therapeutic strategy for Alzheimer's disease: A comprehensive review. Ageing Research Reviews. 2024; 99: 102393.
[13] Pei J, Palanisamy CP, Jayaraman S, Natarajan PM, Umapathy VR, Roy JR, Thalamati D, Ahalliya RM, Kanniappan GV, Mironescu M. A comprehensive review on starch-based Sustainable Edible Films Loaded with Bioactive Components for Food Packaging. International Journal of Biological macromolecules. 2024; 274 (Part-1): 133332.
[14] Palanisamy CP, poompradub S, Sansanaphongpricha K, Subramani K, Sonsudin F. Increased expression levels of PDGF and VEGF magnify the wound healing potential facilitated by biogenic synthesis of silver nanoparticles. Nano-Structures & Nano-Objects. 2024; 39: 101236.
[15] Pei J, Palanisamy CP, Jayaraman S, Natarajan PM, Umapathy VR, Roy JR, Thalamati D, Ahalliya RM, Kanniappan GV, Mironescu M. Proteomics Profiling of Extracellular Vesicle for Identification of Potential Biomarkers in Alzheimer's Disease: A Comprehensive Review. Ageing Research Reviews. 2024; 99: 102359.
[16] Xi J, Wang T, Xian P, Liu X, Du M, Yang H, Palanisamy CP, Lin W, Long Q. Proteomic insights uncover enhanced neurotherapeutic potential in conditioned mesenchymal stem cell-derived extracellular vesicles. Extracellular Vesicle. 2024; 3: 100037.
[17] Pei J, Natarajan PM, Umapathy VR, Swamikannu B, Sivaraman NM, Krishnasamy L, Palanisamy CP. Advancements in the synthesis and functionalization of zinc oxide-based nanomaterials for enhanced oral cancer therapy. Molecules. 2024; 29(11): 2706.
[18] Gatasheh MK, Natarajan SR, Krishnamoorthy R, Alsulami TS, Rajagopal P, Palanisamy CP, Veeraraghavan VP, Jayaraman S. Molecular analysis to identify novel potential biomarkers as drug targets in colorectal cancer therapy: an integrated bioinformatics analysis. Molecular and Cellular Oncology. 2024; 11(1): 2326699.
[19] Pei J, Yan Y, Jayaraman S, Rajagopal P, Natarajan PM, Umapathy VR, Gopathy S, Roy JR, Sadagopan CS, Thalamati D, Palanisamy CP, Mironescu M. A review on advancements in the application of starch-based nanomaterials in biomedicine: Precision drug delivery and cancer therapy. International Journal of Biological Macromolecules. 2024; 130746.
[20] Pei JJ, Yan Y, Palanisamy CP, Jayaraman S, Natarajan PM, Umapathy VR, Gopathy S, Roy JR, Sadagopan JC, Thalamati D, Mironescu M. Materials-based drug delivery approaches: Recent advances and future perspectives. Green Processing and Synthesis. 2024; 13: 20230094.
[21] Pei JJ, Deng W, Liu Y, Guo Y, Chen J, Abdu H, Khan MR, Palanisamy CP, El-Aty AM. A Comprehensive Review of Cornus officinalis: Health Benefits, Phytochemistry, and Pharmacological Effects for Functional Drug and Food Development. Frontiers in Nutrition. 2023; 10: 1309963.
[22] Alugoju P, Palanisamy CP, Anthikapalli NVA, Jayaraman S, Prasanskulab A, Chuchawankul S, Dyavaiah M, Tencomnao T. Exploring the anti-aging potential of natural products and plant extracts in budding yeast Saccharomyces cerevisiae: A review. F1000Research. 2023; 12: 1265.

[23] Lavanya M, Krishnamoorthy R, Alshuniaber MA, Manoharadas S, Palanisamy CP, Veeraraghavan VP, Jayaraman S, Rajagopal P, Padmini R. Formulation, characterization and evaluation of gelatin-syringic acid/zinc oxide nanocomposite for its effective anticancer, antioxidant and anti-inflammatory activities. Journal of King Saud University-Science. 2023; 35: 102909.
[24] Palanisamy CP, Poompradub S, Sansanaphongpricha K, Jayaraman S, Subramani K, Sonsudin F. Biosynthesis of silver nanoparticles (AgNPs) using ethanolic extract of Nigella sativa (L.) seeds promotes wound healing via PDGF and VEGF signalling pathways activation. Biocatalysis and Agricultural Biotechnology. 2023; 54: 102970.
[25] Prasad M, Jayaraman S, Natarajan SR, Veeraraghavan VP, Krishnamoorthy R, Gatasheh MK, Palanisamy CP, Elrobh M. Piperine modulates IR/Akt/GLUT4 pathways to mitigate insulin resistance: Evidence from animal and computational studies. International Journal of Biological Macromolecules. 2023; 253: 127242.
[26] Palanisamy CP, Pei JJ, Phaniendra A, Venkata AAN, Jayaraman S, Veeraragahavan VP, Sridevi G, Roy JR, Janaki CS, Thalamati D, Mironescu M, Luo Q, Chai Y, Long Q. New Strategy of Neurodegenerative Disease Treatment with Extracellular Vesicles (EVs) Derived from Mesenchymal Stem Cells (MSCs). *Theranostics*. 2023; 13(12):4138-4165. doi:10.7150/thno.83066.
[27] Palanisamy CP, Phaniendra A, Jayaraman S, Poompradub S. *Nigella sativa* L. seed extracts promotes wound healing progress by activating VEGF and PDGF signalling pathways: *An in vitro* and *in silico* study. *F1000 Research*. 2023; 12: 436.
[28] Palanisamy CP, Cui B, Zhang H, Gunasekaran VP, Ariyo A, Jayaraman S, Veeraraghavan V, Rajagopal P. A critical review on starch-based electrospun nanofibrous scaffolds for wound healing application. International Journal of Biological Macromolecules. 2022; 222 (Part: B): 1852-1860.
[29] Monisha P, Ponnulakshmi R, Nalini D, Vishnu P V, Palanisamy CP, Cui B, Shankargouda P, Selvaraj J. A comprehensive review on high fat diet-induced diabetes mellitus: An epigenetic view. The Journal of Nutritional Biochemistry. 2022; 2022: 109037.
[30] Monisha P, Selvaraj J, Mohamed AE, Mohamed E, Mosaab AEA, Vishnu PV, Srinivasan V, Vidhya RU, Shazia FJH, Kalaiselvi K, Durairaj S, Palanisamy CP, Surapaneni K M, Ponnulakshmi R. A Comprehensive review on therapeutic perspectives of phytosterols in insulin resistance: A mechanistic approach. Molecules. 2022; 27(5): 1595.
[31] Natarajan PM, Swamikannu B, Sivaraman NM, Stylin AGSQ. Prevention of Oral Cancer: A Comprehensive Guide. Journal of Pharmacy and Bioallied Sciences. 2024; 16(5): S4239-S4241.
[32] Umapathy V, Dhanavel A, Kesavan R, Natarajan PM, Bhuminathan S, Vijayalakshmi P. Anticancer Potential of the Principal Constituent of Piper nigrum, Piperine: A Comprehensive Review. Cureus. 2024; 16(2): e54425.
[33] Umapathy VR, Swamikannu B, Natarajan PM, Devi R, Nandini MS, Vimalarani, Vijayalakshmi P. In Silico Molecular Docking of Ocimum sanctum Phytochemicals: Targeting Key Biomarkers in Oral Cancer. Journal of Pharmacy and Bioallied Sciences. 2024; 16(5): S4792-S4799.
[34] Natarajan PM, Bhuminathan S, Rajan R, Bindu K, Loganathan K, Veerakumar R. The Crucial Role of Smoking Cessation in Preventing Oral Cancer. Journal of Pharmacy and Bioallied Sciences. 2024; 16(5): S4245-S4247.
[35] Swamikannu B, Umapathy VR, Natarajan PM, Nandini MS, Stylin AGSQ, Vimalarani V, Rajinikanth S. Unlocking the Therapeutic Benefits of Artemisia Annua: A Comprehensive Overview of its Medicinal Properties. Journal of Pharmacy and Bioallied Sciences. 2024; 16(5): S4248-S4253.
[36] Natarajan PM. Computational Studies on Recent Congeners of Fluoroquinolones and Nitroimidazoles for Their Use in Periodontal Therapy. Journal of Pharmacy and Bioallied Sciences. 2024; 16(5): S4731-S4740.
[37] Yadalam PK, Arumuganainar D, Natarajan PM, Ardila CM. Artificial intelligence-powered prediction of AIM-2 inflammasome sequences using transformers and graph attention networks in periodontal inflammation. Scientific Reports. 2025; 15: 8733.
[38] Yadalam PK, Chatterjee S, Natarajan PM, Ardila CM. Comparison of light gradient boosting and logisti c regression for interactomic hub genes in Porphyromonas gingivalis and Fusobacterium nucleatum-induced peri odontitis with Alzheimer's disease. Frontiers in Oral Health. 2025; 6:1463458.
[39] Natarajan PM, Bhuminathan S, Leela B, Bindu K, Loganathan K, Ramachandran V. Smoking and its Role in Oral Cancer. Journal of Pharmacy and Bioallied Sciences 16(5): S4242-S4244.
[40] Yadalam PK, Natarajan PM, Ardila CM. Variational graph autoencoder for reconstructed transcriptomic data associated with NLRP3 mediated pyroptosis in periodontitis. Scientific Reports. 2025; 15: 1962.
[41] Pei JJ, Perumal NC, Meng P, Long Q, Palanisamy CP. AI-assisted FTIR spectroscopic profiling of exosomes: Emerging frontiers in early detection of Alzheimer's disease. Ageing Research Reviews. 2026; 103311.
[42] Raja FSD, Abraham L, Rangasamy K, Saikia K, Rathankumar AK, Mironescu M, Mironescu I, Palanisamy CP, Kanniappan GV. Next-Generation Microbiome Therapeutics: Psychobiotics and Fecal Microbiota Transplants (FMT) for Mental Health Treatment. Frontiers in Cellular and Infection Microbiology. 2026; 16: 1719357.
[43] Subramani K, Srinivasan S, Shanmugam P, Palanisamy CP, Sonsudin F, Poompradub S. Sustainable phytochemical mediated-ZnO nanoparticles derived from Crescentia cujete for toxicological evaluation and

multifunctional environmental applications. Environmental Nanotechnology, Monitoring & Management. 2026; 26: 101180.
[44] Kunamalla RP, Panagal M, Palanisamy CP. Green-engineered multiscale starch/PVA nanofibrous scaffolds embedded with CuO nanoparticles from Sargassum ilicifolium for potent antimicrobial performance. Genetics and Molecular Research. 2026; 25(13s): 1-9.
[45] Dharmaprakash S, Gunasekaran VP, Sivaramakrishnan R, Kanniappan GV, Jayaraman S, Mironescu M, Rajabathar JR, Mironescu ID, Palanisamy CP. Marine macroalgae-mediated ultrasonic-assisted green synthesis of CuO nanoparticles embedded in starch/PVA electrospun nanoscaffolds for in vitro α-amylase and α-glucosidase inhibitory activity. Scientific Reports. 2026; 16: 26243.
[46] Surendran N, Chandrasekaran G, Raju MV, Chandrasekaran MK, Ahalliya RM, Palanisamy CP, Kanniappan GV, Arcot R, Alharbi NS, Thiruvengadam M. Anti-inflammatory potential of ethanolic extract of Maranta arundinacea L.: Insights from COX-2 modulation and oxidative stress analysis. South African Journal of Botany. 2026; 195: 142-151.
[47] Pei J, Senthilkumar MV, Hessini K, Subramaniyam S, Sivaramakrishnan R, Kanniappan GV, Jayaraman S, Palanisamy CP. Green fabrication of starch/PVA/CuO nanoscaffolds using marine macroalgae extract for enhanced anti-inflammatory activity. Sustainable Chemistry and Pharmacy. 2026; 51: 102397.
[48] Balasubramanian V, Loganathan L, Muthuswamy K, Viswanathan TM, Raju MV, Chandrasekaran MK, Ahalliya RM, Poorasamy J, Palanisamy CP, Dominic S, Kanniappan GV. Anticancer therapeutic efficacy of PEGylated β-galactosidase from Aspergillus terreus in DMBA-induced breast cancer: Toxicological, molecular and histopathological evaluation in Wistar rats. International Journal of Biological Macromolecules. 2026; 360: 151856.
[49] Jayaraman S, Eswaran A, Rajagopal P, Palanisamy CP, Veerakumar P, Veeraraghavan VP, Sirasanagandla SR. Neuroendocrine-associated epigenetic factors in cellular senescence: mechanisms and therapeutic implications. Biogerontology. 2026; 27(2): 64.
[50] Jayakumar M, Senthil P, Suganthirababu P, Ramalingam V, Palanisamy CP. Longitudinal effects of body weight supported gait training on functional gait recovery after stroke: A pilot randomized controlled trial. Genetics and Molecular Research. 2026; 25(12s): 2026.
[51] Ponnusamy B, Rajagopal P, Palanisamy CP, Veeraraghavan VP, Jayaraman S. Mechanistic Exploration of the anticancer activity of Justicia adhatoda Plant Leaf Ethanolic Extract against Colon Cancer Cells: An in silico and in vitro Approach. Asian Pacific Journal of Cancer Prevention. 2026; 27(3): 1069-1080.
[52] Pei J, Saran VS, Sivaramakrishnan R, Kanniappan GV, Pandurangan V, Jayaraman S, Dhayalan VK, Mironescu M, Mironescu ID, Palanisamy CP. Ultrasonic-assisted, Sargassum ilicifolium (brown marine macroalgae)-mediated biogenic synthesis of CuO nanoparticles incorporated in starch/PVA electrospun nanoscaffolds: In vitro safety and antioxidant efficacy assessment. Bioorganic Chemistry. 2026; 173: 109679.
[53] Raj MAPA, Subramaniyam S, Kanniappan GV, Jayaraman S, Palanisamy CP. Sustainable fabrication of starch/PVA/CuO electrospun nanoscaffolds from Turbinaria ornata (marine macroalgae) extract: Physicochemical characterization and antidiabetic evaluation. Kuwait Journal of Science. 2026; 53(2): 100545.
[54] Pei J, Ganesh NS, Subramaniyam S, Sivaramakrishnan R, Kanniappan GV, Jayaraman S, Palanisamy CP. Sustainable fabrication of starch/PVA/CuO electrospun nanoscaffolds from Padina tetrastromatica (Brown macroalgae) extract: Physicochemical characterization and antidiabetic assessment. Sustainable Chemistry One World. 2026; 9: 100195.
[55] Sakthiraj A, Sivaramakrishnan R, Subramaniyam S, Kanniappan GV, Pandurangan V, Jayaraman S, Dhayalan VK, Mironescu M, Mironescu ID, Palanisamy CP. Starch/PVA electrospun nanoscaffolds loaded with ultrasonic-assisted green-synthesis of CuO nanoparticles from marine macroalgae (Gracilaria corticata) extract: Cytotoxicity and antioxidant analysis. Chemical Physics Impact. 2026; 12: 101018.
[56] Raju M, Chandrasekaran MK, Loganathan L, Ahalliya RM, Mironescu M, Mironescu ID, Palanisamy CP, Kanniappan GV. Lipid remodeling and ferroptosis in phosphatidylcholine-mediated tumor–stroma crosstalk. Frontiers in Molecular Biosciences. 2026; 13: 1742305.
[57] Kunamalla R, Panagal M, Palanisamy CP. Biogenic synthesis and fabrication of starch/PVA/CuO electrospun nanoscaffolds from Sargassum ilicifolium (brown marine macroalgae) extract for anticancer activity on HT-29 and MCF-7 cancer cells. Biocatalysis and Agricultural Biotechnology. 2026; 72: 103923.
[58] Pei J, Govindaraj H, Sivaramakrishnan R, Kanniappan GV, Pandurangan V, Dhayalan VK, Mironescu M, Mironescu ID, Jayaraman S, Palanisamy PC. Sustainable fabrication of biopolymer-based (starch/PVA) nanoscaffolds loaded with green-synthesized CuO nanoparticles from Sargassum wightii (marine macroalgae): Cytocompatibility and antioxidant activity. Biomaterials Advances. 2026; 182: 214660.
[59] Pei J, Perumal NC, Meng P, Long Q, Palanisamy CP. Extracellular vesicle-based biosensors for Alzheimer's disease: A new frontier in precision diagnostics. Ageing Research Reviews. 2026; 113: 102904.
[60] Shree P, Sivaramakrishnan R, Kanniappan GV, Pandurangan V, Jayaraman S, Dhayalan VK, Mironescu M, Mironescu ID, Palanisamy CP. Antioxidant and biocompatible CuO-starch/PVA nanoscaffolds via ultrasonic green synthesis using Turbinaria conoides (brown marine macroalgae). Medicine in Drug Discovery. 2025; 28: 100238.
[61] Gong J, Lin J, Guan T, Pei J, Palanisamy CP, El-AtyFrom AMA. selenium tolerance to nanoplastic antagonism: Comprehensive characterization of L. casei SNUT1 and its extracellular vesicle–nanoselenium

complex. Food Bioscience. 2025; 74: 107749.
[62] Poochi SP, Sundarraj R, Raju MV, Chandrasekaran MK, Ahalliya RM, Palanisamy CP, Kanniappan GV, Kondapavuluri BK, Thiruvengadam M. Harnessing Nature: Computational and Experimental Insights Into *Ipomoea obscura* Metabolites for Bladder Cancer Therapy. Chemistry and Biodiversity. 2025; 0: e00909.
[63] Dugganaboyana GK, Kannankumar MKG, Shivaramakrishna S, Raju MV, Chandrasekaran MK, Ahalliya RM, Panneerselvam N, Palanisamy CP, Kanniappan GV. Phytochemical insights, antioxidant activity and therapeutic potential of Cassia senna against prostate cancer in Wistar albino rats. Discover Applied Sciences. 2025; 7:1206.
[64] Natarajan SR, Krishnamoorthy R, Alshuniaber MA, Gatasheh MK, Rajagopal P, Veeraraghavan VP, Palanisamy CP, Jayaraman S. KDM1A Facilitates Oncogenic Potential in Colorectal Cancer Progression Through the Activation of AXIN/GSK3β/β-Catenin Signaling Pathways: Evidence From Integrated Transcriptomics and In Vitro Studies. The Journal of Gene Medicine. 2025; 27(11): e70053.
[65] Guan T, Gong J, Lin J, Palanisamy CP, Jinjin Pei J, El-Aty AMA. Machine learning-driven multimodal optimization of selenium biotransformation and flavor profiling in fermented apple–Yacon functional beverages. Innovative Food Science & Emerging Technologies. 2025; 105: 104198.
[66] Natarajan SR, Krishnamoorthy R, Alshuniaber MA, Alsulami TS, Gatasheh MK, Rajagopal P, Palanisamy CP, Govindan R, Veeraraghavan VP, Jayaraman S. ABCE1 facilitates tumour progression via aerobic glycolysis and inhibits cell death in human colorectal cancer cells through the p53 signalling pathway. Scientific Reports. 2025; 15: 24674.
[67] Huang Y, Guo H, Liu Y, Jin W, Palanisamy CP, Pei J, Oz F, El-Aty AMA. Effects of Natural Polysaccharides on the Gut Microbiota Related to Human Metabolic Health. Molecular Nutrition & Food Research. 2025; 69:e202400792.
[68] Poornima K, Meenakshi K.C, Manikandan V.R, Shankari G, Prabhu D, Rathi M.A, Palanisamy CP, Balaji R, Gopalakrishnan V.K. Exploring the anticancer potential of Jerantinine A from *Tabernaemontana coronaria* against prostate, breast, and ovarian cancers: A computational approach. *Journal of Complementary and Integrative Medicine*, 2025 22(2): 363–372.
[69] Palanisamy CP, Poompradub S, Sansanaphongpricha K, Jayaraman S, Subramani K. Faridah Sonsudin gGreen synthesis of Nigella sativa-mediated silver nanoparticles for enhanced antibacterial activity and wound healing: Mechanistic insights and biomedical applications. Environmental Nanotechnology, Monitoring & Management. 2025; 24: 101085.
[70] Surendran N, Raju MV, Chandrasekaran MK, Ahalliya RM, Palanisamy CP, Chandrasekaran G, Kanniappan GV. Physicochemical characterization of starch from Maranta arundinacea L.(arrowroot) rhizomes and its inhibition of COX-2: In vivo validation. Bioactive Carbohydrates and Dietary Fibre. 2025; 33: 100465.
[71] Natarajan PM, Umapathy VR, Murali A, Swamikannu B. (2022). Computational Simulations of Identified marine-derived Natural Bioactive Compounds As Potential Inhibitors of Oral Cancer. Future Science OA. 2022; 8(3).
[72] Natarajan PM, Umapathy VR. Role of transcriptomics in the study of oral cancer. Frontiers in Oral Health. 2025; 6:1524364.
[73] Vidhyarekha U, Natarajan PM, Bhuminathan S, Sabarinathan J, Suba R, Vijayalakshmi P. Role of artificial intelligence in Oral Cancer. Advances in Public Health. 2024. 2024: 3664408.
[74] Ganesan A, Kumar NG, Natarajan PM, Gauthaman J. Automated classification of elongated styloid processes using deep learning models-an artificial intelligence diagnostics. Frontiers in Oral Health. 2025; 5: 1424840.
[75] Umapathy VR, Natarajan PM, Swamikannu B. Regenerative Strategies in Dentistry: Harnessing Stem Cells, Biomaterials and Bioactive Materials for Tissue Repair. Biomolecules. 2025; 15: 546.
[76] Natarajan PM. Dental Bioinformnatics-Current Scope and Future perspectives. Research Journal of Pharmacy and Technology. 2022;15(5):2351-6.
[77] Ganesan A, Kumar NG, Natarajan PM. Solanum trilobatum leaf extract-derived silver nanoparticles downregulate the PI3K/AKT/mTOR signaling pathway and attenuate oral squamous cell carcinoma cell proliferation. Journal of Herbmed Pharmacology. 2024; 13(2): 300-307.
[78] Perumal MKK, Renuka RR, Subbiah SK, Natarajan PM. Artificial intelligence-driven clinical decision support systems for early detection and precision therapy in oral cancer: a mini review. Frontiers in Oral Health. 2025; 6: 1592428.
[79] Ramesh E, Ganesan A, Lakshmi KC, Natarajan PM. Artificial intelligence-based diagnosis of oral leukoplakia using deep convolutional neural networks Xception and MobileNet-v2. Frontiers in Oral Health. 2025; 6: 1414524.
[80] Ganesan A, Kumar NG, Natarajan PM. Anticancer activity of silver nanoparticles synthesized from aqueous leaf extract of Solanum trilobatum (Purple fruit pea eggplant) on human oral cancer cells. Journal of Herbmed Pharmacololgy. 2024; 13(2): 260-268.